TWELFTH EUROPEAN ROTORCRAFT FORUM

Paper No. 33

INVESTIGATION OF HELICOPTER TWIN-ROTOR CHARACTERISTICS

H. Azzam and P. Taylor

Department of Aeronautics and Astronautics
University of Southampton, Southampton, U.K.

September 22 - 25, 1986

Garmisch-Partenkirchen
Federal Republic of Germany

Deutsche Gesellschaft für Luft- und Raumfahrt e. V. (DGLR)
Godesberger Allee 70, D-5300 Bonn 2, F.R.G.

INVESTIGATION OF HELICOPTER TWIN-ROTOR CHARACTERISTICS

H. Azzam, Research Fellow, Southampton University
P. Taylor*, Southampton University, U.K.

Abstract

The general application of the reported wake models to the interference problems between two rotors is restriced. The free convection of a limited number of revolutions of the tip vortex trajectory is only considered in the free wake models to reduce the computational costs. Meanwhile, the far wake is either ignored or prescribed by using a vortex ring or a helical wake of constant radius. The objective of this paper is to demonstrate the important effects of the far wake structure on the twin-rotor behaviour. This leads to the proposed prescribed wake model. This model is found to describe the performance of coaxial, nonoverlapped tandem and twin-tail rotors adequately. The flapping angles of the nonoverlapped tandem were found to be reasonably predicted.

Notation

a	:	The local lift curve slope
b	:	Number of blades
c	:	Blade chord, metres
C_T	:	Thrust coefficient, $= 2T/(\rho A V_T^2)$
C_q	:	Torque coefficient, $= 2Q/(\rho A R V_T^2)$
C_{qd}	:	Torque coefficient, $= 2Q_d/(\rho A R V_T^2)$
e	:	Flapping hinge offset, nondimensionalized w.r.t. R
g	:	Out of plane mode shape, metres
K_d	:	Induced power factor in hover, $= 2C_{qd}/C_T^{1.5}$
m	:	Mass per unit length of the blade, kilograms/metre
n	:	Momentum contraction ratio
n_e	:	Effective contraction ratio
Q	:	Rotor torque, Newtons-metre
Q_d	:	The difference between the torque of the rotor at certain advance ratio and the torque of the same rotor with zero collective pitch angle at the same advance ratio, Newtons-metre
R	:	Rotor radius, metres
T	:	Rotor thrust, Newtons
V_T	:	Rotor tip speed, metres/second
Γ	:	Strength of the bound circulation, metres^2/second
γ	:	Strength of a trailing vortex, metres^2/second
ε	:	Root cut out, nondimensionalized w.r.t. R
η	:	Time dependent flapwise coordinate, radians
θ	:	Local pitch angle, radian
λ_{io}	:	Momentum induced velocity in forward speed, nondimensionalized w.r.t. V_T
λ	:	Tip vortex contraction rate
λ_1, λ_2	:	Tip vortex settling rates, nondimensionalized w.r.t. V_T
μ	:	Local velocity of the air, nondimensionalized w.r.t. V_T
μ_T	:	Tangential component of the local velocity of the air, nondimensionalized w.r.t. V_T
μ_{N2}	:	Normal component of the local velocity of the air which does not include the effect of the near wake, nondimensionalized w.r.t. V_T
ν	:	Flapwise natural frequency, nondimensionalized w.r.t. Ω
ρ	:	Air density, kilograms/metre^3
Ω	:	Rotor rotational speed, radians/second

*Presently at Westland PLC, Helicopter Division

1 - Introduction

The momentum theory provides the simplest mathematical model applicable to the prediction of twin-rotor performance; Stepniewski (1955, ref. 1 and 1979, ref. 2). In ref. 3, the momentum theory is used to explain the main features of twin-tail rotor whose discs are not necessarily parallel to each other. On the other hand, several wake models have been developed to study the twin rotor behaviour. For example, the wake models of Sadler (1971, ref. 4), Baskin et al (1976, ref. 5) and Johnson (1981, ref. 6) are applicable to twin-rotor configurations. However, these models have not been validated by checking the capability of predicting the twin rotor performance. Cheeseman (1958, ref. 7) combined the actuator disc theory and a horseshoe vortex pattern to study the effect of one rotor on another. Cheeseman applied his model to the case of nonoverlapped tandem rotors and compared the theoretical results with the experimental data reported by Dingledein (1954, ref. 8). The agreement between the theory and the test was reasonably good. Nevertheless, this model was developed to only provide the general performance characteristics of the twin rotor. Harrington (1951, ref. 9) suggested that the performance of a coaxial rotor can be investigated by considering a model for a single equivalent rotor. However, the behaviour of the coaxial rotor is influenced by the axial separation and phase angle between the rotors. Therefore, various wake models have been developed to study the detailed characteristics of the coaxial rotor; e.g. Nagashima (1981, ref. 10), Andrew (1983, ref. 11) and Zimmer (1985, ref. 12). Nagashima approximated the tip vortex of each blade to vortex rings and used the free wake method to study the performance of the coaxial rotor in hover. The basic feature of Andrew's model is that the tip vortex of each blade is used to calculate the induced velocities along the blades. Then, the values of induced velocities are increased by certain values as described in ref. 11. Zimmer used a prescribed wake model to calculate the induced velocities. Then, the momentum theory was utilized to correct the calculated induced velocities.

As demonstrated in ref. 13, the prescribed wake model "RWAKE" describes the behaviour of a single rotor adequately. Meanwhile, the induced velocities produced by the model have not been corrected. This is an indication that the wake of the single rotor is reasonably simulated. The objective of this paper is to demonstrate the feasibility of extending this model to investigate the twin rotor configurations by considering the important effects of the far wake structure.

2 - The "RWAKE" model

A brief description of the "RWAKE" model will be presented. Detailed description and validation of this model for a single rotor are reported in ref. 3 and ref. 13.

The near interactive wake is assumed to exist for a number of degrees azimuth corresponding to the time required for the rolling up process of the tip vortex to complete. This wake is represented by straight line vortex filaments positioned midway between the points at which the bound circulations are calculated. The strength of these filaments are related to the blade loading by using the lifting line theory to obtain:

$$\Gamma_i = 0.5\, c\, a_i\, V_T \left\{ \mu_i [\theta_i + tan^{-1}(\mu_{N2}/\mu_T)] - \frac{1}{V_T} \sum_{j=1}^{b(n-1)} \sigma_{i,j}\, \gamma_j \right\} \qquad (1)$$

where:

- "Γ_i" is the bound circulation at the ith control point
- "a_i" is the local lift curve slope
- "θ_i" is the local pitch angle
- "$\sigma_{i,j}$" is the influence coefficient of the jth trailing vortex at the ith control point
- "γ_j" is the strength of the jth trailing vortex
- "μ_i" is the local velocity of the air
- "μ_T" is the tangential component of the local velocity of the air
- "μ_{N2}" is the normal component of the local velocity of the air which includes the induced velocities due to the tip vortex, the root vortex and any external field, and does not include the induced velocity due to the near interactive wake.

The tip vortex trajectory is prescribed for any flight regime by using the momentum theory to generalize the experimental results of a rotor in hover reported by Kocurek and Tangler (1977, ref. 14). The instantaneous radius of the tip vortex; "r_i" is calculated from:

$$r_i/R = \sqrt{n_e} + (1 - \sqrt{n_e})\, e^{-\lambda \psi_w} \tag{2}$$

where: "ψ_w" is the wake azimuth angle relative to the blade
"λ" is the contraction rate; ref. 14.
"n_e" is the effetive contraction ratio

The effective contraction ratio "n_e" at any forward speed is assumed to be a linear function of the momentum contraction ratio "n":

$$n = V/W \tag{3}$$

$$n_e = 0.7832\, n + 0.2168 \tag{4}$$

where: "V,W" are the resultant velocities at the rotor disc and far downstream based on momentum theory.

Then, the settling rates of the tip vortex; "λ_1, λ_2" at any forward speed are related to the contraction ratios through the following equations:

$$\lambda_1 = \lambda_{io}\left[1 - K_1\left(\frac{n_e}{n} - 1\right)\right] \tag{5}$$

$$\lambda_2 = \lambda_{io}\left[1 - K_2\left(\frac{n_e}{n} - 1\right)\right] \tag{6}$$

where: "λ_{io}" is the momentum induced velocity.

The constant "K_1" and "K_2" are selected such that the settling rates correspond to the experimental values in hover which are reported in ref. 14. After the point of maximum contraction the wake is allowed to expand up to one radius.

The tip vortex strength is assumed to be equal to the average of the blade circulation "Γ_a":

$$\rho \Gamma_a(\psi) \int_{\varepsilon}^{1} (x-e)\, \mu_T\, dx = \Omega \sum_k \left(\eta_k^{\cdot} + \nu_k^2\, \eta_k\right) \int_0^{1-e} m\, g_k(x)\, x\, dx \tag{7}$$

where: "ρ" is the air density
"x" is nondimensional radial coordinate
"e" is the flapping hinge offset
"ε" is the root cut out
"g_k" is the kth flapwise mode shape
"η_k" is the kth time dependent coordinate
"ν_k" is the associated natural frequency
"m" is the mass per unit length

The strength of the root vortex is equal and opposite to that of the tip vortex.

3 - Twin-Rotor Wake Model

The direction of rotation and the position of each rotor along with the phase angle between the corresponding blades of the two rotors are input to the program. These parameters along with the flapping angles are utilized to calculate the instantaneous positions of the control points of each rotor viewed from the wake of the other rotor. The induced velocity components produced by the wake of one rotor at the control points of the other rotor are regarded as an external velocity field. Then, the bound circulations of each blade are evaluated; equation (1). The strength of each tip vortex is calculated by considering the first flapwise mode only; equation (7). The twin-rotor is trimmed such that a total required value of the thrust is produced. Then, each rotor is considered to produce a specified value of thrust or both rotors are considered to absorb the same amount of power. The consistency between the bound circulations, induced velocities and dynamic response of both rotors can be achieved by adopting an appropriate algorithm. The algorithm presented

hereafter is for a twin-rotor trimmed such that each rotor produces a specified value of thrust, and is used in order to implement the software of the "RWAKE" model directly;

a - Initialization

The thrust coefficient and the cyclic control angles of each rotor are used to calculate the momentum induced velocity and initial values for the collective pitch and flapping angles. This information is used to establish the initial wake geometry and the strength of the tip vortex of each rotor. The direction of rotation and the position of each rotor along with the phase angle between the two rotors and the flapping angles are used to define the initial instantaneous position of the control points of rotor 1 relative to the axes of rotor 2. Then, the velocity field produced by the root vortex and the tip vortex of rotor 2 at the control points of rotor 1 is calculated at each time step.

b - Rotor 1

1 - The induced velocity field produced by the wake of rotor 2 at the control points of rotor 1 is considered to be an external field which will not change in this block of calculations.

2 - The current values of the flapping angles are used to establish the wake geometry and the tip vortex strength of rotor 1.

3 - The contribution of the root vortex and tip vortex of rotor 1 to the induced velocities at the control points of the same rotor are calculated and added to the external velocity field.

4 - The bound circulations of this rotor are calculated; equation (1). Thus, the contribution of the near wake of rotor 1 to the induced velocities of the same rotor is obtained.

5 - The velocity field produced by the wake of rotor 1 at the control points of rotor 2 is evaluated.

6 - The total values of the induced velocities at the control points of rotor 1 along with the current value of the collective pitch angle are used to calculate the thrust of this rotor. The value of the thrust is checked and the collective pitch angle is adjusted to obtain the required thrust without changing the induced velocity profile.

7 - The bound circulations of rotor 1 are recalculated for the new value of the collective pitch angle. Then the contribution of the near wake to the induced velocities is updated.

8 - New estimates of the local flapping angles of rotor 1, which are consistent with the current total induced velocity profile are evaluated.

9 - The process is repeated from step 6 until the values of the collective pitch angle, flapping angles and the bound circulations of rotor 1 have all converged for the current external velocity field produced by rotor 2.

c - Rotor 2

This block of calculations reads similar to the previous block if the word "rotor 1" is interchanged with "rotor 2".

The calculation is restarted from block b until the collective pitch angles, the flapping angles, the bound circulations and the external velocity fields of both rotors have all converged.

It is worth emphasizing that the induced velocities at each control point are calculated from the wake of the twin rotor. It is required then, to establish the tip vortex trajectory which may result in reasonable values of the induced velocities without the need of any corrections.

4 - The Wake Geometry of the Twin Rotor

For twin rotor configurations, the flow visualization of the tip vortex is not as extensively documented as for a single rotor. Therefore, prescribing the wake geometry of a twin rotor seems to be a formidable task. The wake structure of a tandem rotor is not necessarily similar to that of a coaxial rotor. The discs of the twin-tail rotor are not parallel to each other. Hence, the tip vortex trajectory of the upstream rotor is expected to be modified by the velocity field of the downstream rotor, especially in the region adjacent to the downstream rotor. Furthermore, there is no available experimental data or empirical formulae which describe the structure of the far wake of a single rotor. Therefore, as a first attempt, the wake of each rotor is assumed to be exactly the same as

described in section 2. It is required then to specify the parameters by which the tip vortex trajectory is prescribed. Two cases are considered:

In the first case, the wake of each rotor is completely influenced by the wake of the other rotor. This is an approximation of the coaxial rotor with small axial separation. In this case, the contraction and the settling rates; "λ, λ_1, λ_2" of the tip vortex of each blade are calculated by substituting the values of the total thrust coefficient and the total number of blades of the twin-rotor into the empirical formulae of ref. 14 and by using the analysis of section 2. This model is validated by the flow visualization of the coaxial rotor reported by Saito (1981, ref. 15). It is found that the contraction and settling rates of the coaxial rotor are very close to those of an equivalent single rotor.

In the second case, the contraction and settling rates are calculated for each rotor by using its thrust coefficient and number of blades. Thus, the contraction and settling rates of this case are less than those of the first case. However, the average value of the instantaneous induced velocities produced by the wake of each rotor at the control points of the other rotor (the external velocity field) are used as an additional axial settling rate. This average is calculated within block b and block c of the algorithm described in the previous section. This case is assumed to be an approximation of nonoverlapped tandem and twin-tail rotor configurations. The validity of these models can be now examined by comparing the theoretical results to the available experimental data.

The experimental results of the coaxial rotor presented in Figure 1 are those reported by Harrington (1951, ref. 9). The coaxial rotor consisted of two 7.62 metres diameter, two-bladed rotors. Each blade was rigidly restrained in flapping motion as well as in the plane of rotation. The blades were untapered in plane form (chord = 0.4572 metres) and tapered in thickness ratio. The axial separation between the two rotors was 0.6096 metres (= 0.16 R). Figure 1 indicates that the "RWAKE" model does not describe the performance of the coaxial rotor adequately. At this point, it may be argued that the contraction and settling rates are in error. However, the "RWAKE" model was found to describe the behaviour of a single rotor adequately. Meanwhile, the flow visualization test reported by Saito indicated that the chosen rates are not far from reality. Then, the phenomenon to be examined is either the blade-vortex interaction or the structure of the far wake. A simplified way of investigating the effect of the blade-vortex interaction is to vary the value of the equivalent core radius of the tip vortex. Nevertheless, for this coaxial case, it was found that the value of the core radius proposed in ref. 13 is an appropriate choice for both the numerical stability and the smooth variation of the power with thrust.

5 - The Far Wake Representation

The flow visualization test of a hovering rotor conducted by Kocurek and Tangler (1977, ref. 14) indicated that the wake undergoes a continuous expansion after the point of maximum contraction. This point was defined by the fourth passage of the tip vortex beneath the blade. The expanded wake will be denoted from here on by the far wake. The settling rate of the far wake has been found to be less than "λ_2". However, it was difficult to measure an exact value (or values) of this rate because the far wake is characterized by instability, vortex core breakdown and diffusion; ref. 14. Kocurek and Tangler modelled the effect of the far wake in hover by a vortex ring centred on the axis of rotation at an axial level corresponding to the fourth passage of the tip vortex beneath the reference blade. The strength of the vortex ring was chosen to be four times that of the tip vortex. Pouradier (1981, ref. 16) utilized a similar model, however, the radius of the vortex ring was chosen to be equal to 1.2R. This representation is not valid for twin rotor configurations because the far wake is abruptly truncated and the position of the vortex ring may result in spurious effects on the downstream rotor.

In the "RWAKE" model the far wake is allowed to expand up to one rotor radius only. In the new generation of the model; "RWAKE2" the far wake is allowed to expand continuously and its settling rate is reduced gradually up to a value equal to the momentum induced velocity. The remaining task is the choice of two parameters which describe the rate of expansion of the far wake and the rate of reduction of its settling rate. This task is achieved by changing the values of these parameters and by monitoring the effect of that on the performance of a single rotor in hover. Consequently, a linear expansion of the far wake and an exponential reduction of its settling rate are chosen. The radius of the tip vortex reaches a value of 1.25R at the thirteenth tip vortex passage beneath the reference blade. Meanwhile, the settling rate of the far wake tends to the momentum induced velocity by a rate equal to "$\lambda/6$". The proposed tip vortex trajectory is shown in Figure 2. This simple

representation of the far wake is found to improve the performance of a single rotor in hover at low values of thrust coefficient, Figure 3. Meanwhile the performance of the single rotor at high values of thrust coefficient is found to be slightly influenced. It is found also that the performance of a single rotor in hover deteriorates if the settling rate of the far wake is reduced below the value of the momentum induced velocity. The "RWAKE2" is checked at the speed range to ensure that the far wake parameters are appropriately chosen.

As shown in Figure 4 the agreement between the test and the results of the "RWAKE2" model are reasonable for both single and coaxial rotors. The upstream rotor produces a higher value of thrust compared to the downstream rotor in order to maintain the yawing trim condition; Figure 5.

A comparison between the results of both wake models and the experimental data of a twin-tail rotor in hover; ref. 13 is shown in Figure 6. The results of the "RWAKE2" model are displaying a closer agreement with the test compared to those of the "RWAKE" model. The experimental results of the twin-tail rotor at an advance ratio of 0.02 are compared to the theory and presented in Figures 7 and 8.

The results of the "RWAKE2" model are compared to the experimental data of Huston (1963, ref. 17) for both single and tandem configurations in forward flight. The rotor tested was a two-bladed teetering rotor of 2.324 metres radius and a constant chord of 0.3535 metres. For the tandem configuration, the rotor blades were phased ninety degrees apart. As viewed from above, the upstream rotor rotated clockwise and the rear rotor rotated counter-clockwise. The spacing between hubs was equal to 2.03R. The thrust coefficient of each rotor was equal to .0086. The rotors were trimmed for zero flapping with respect to the shaft. The accuracy of the flapping measurements was 0.25 degrees.

Figures 9 to 11 show the comparison between the theory and the test for a single rotor. The longitudinal flapping angles relative to nonfeathering axes (i.e. the longitudinal cyclic control angles for this trim condition) are reasonably predicted by the "RWAKE2" model. Meanwhile the model overestimates the lateral flapping angle but only at low forward speed. Nevertheless, the accuracy of the measurements as well as the wind tunnel interference effects observed by Huston may explain this. Huston corrected the power for the longitudinal component of the rotor resultant force. This component, or the propulsive force, was corrected for rotor-off tares. Figure 11 shows a comparison between the theoretical power and the total experimental power. The differences between the theory and the test may be attributed to the corrections imposed on the experimental data. For example, the experimental trim conditions were set such that the propulsive power of the tandem rotor is twice that of a single rotor. However, the measured propulsive force of the tandem rotor was found to be higher than twice the value of the single rotor.

The results of the tandem configuration are presented in Figures 12 to 17. Surprisingly, the "RWAKE2" model predicts the flapping angles of the downstream rotor (especially the lateral one) more accurately than it does for the upstream rotor. Meanwhile, the trend of the variation of the power with forward speed is reasonably predicted. The differences between the test and the theory are attributed to the corrections imposed on the experimental data, the accuracy of the measurements and wind tunnel interference effects. For example, an error in the tilt of the rotor disc relative to the wind of 0.25 degrees may result in a considerable change in the required power. The accuracy of the measurements can be easily assessed by comparing the power requirement of the single rotor to that of the upstream rotor.

With reference to these figures it is concluded that the "RWAKE2" model is capable of describing the performance of twin rotor configurations adequately. Further investigations of the tip vortex structure and the geometry of the far wake will result in a further refinement of the model. The important parameters which may need further study are the azimuth angle which defines the point of maximum contraction, the settling rate (or rates) of the far wake, the parameters which describe the expansion of the far wake and, may be, its instability and the tip vortx structure in the far field. Such investigations are very useful not only for twin-rotor applications but also for the various interactional problems between the wake of the main rotor and the other components of the helicopter.

6 - Conclusions

It has been demonstrated that the prescribed wake model described in reference 13 can be extended to study the twin rotor configurations. The far wake was allowed to expand continuously and its settling rate was reduced gradually up to a value equal to the momentum induced velocity. This representation of the far wake was found to improve the predictive capability of the wake model for both single and twin rotor configurations. The wake model was validated by comparing its results to the experimental data of a coaxial, nonoverlapped tandem and a twin-tail rotor.

References

(1) W.Z. Stepniewski — A Simplified Approach to the Aerodynamic Rotor Interference of Tandem Helicopters, Proceedings of the West Coast A.H.S. Meeting, 1955.

(2) W.Z. Stepniewski — Rotary-Wing Aerodynamics, NASA CR 3082, 1979.

(3) H. Azzam — Investigation of Single and Twin Rotor Behaviour, Dissertation Submitted for the Degree of Ph.D., Southampton University, 1986.

(4) S.G. Sadler — Development and Application of a Method for Predicting Rotor Free Wake Positions and Resulting Rotor Blade Airloads, NASA CR 1911, 1971.

(5) V.E. Baskin, L.S. Vil'dgrube, YE.S. Vozhdayev, G.I. Maykapar — Theory of the Lifting Airscrew, NASA TT F-823, 1976.

(6) W. Johnson — Development of a Comprehensive Analysis for Rotorcraft I. Rotor Model and Wake Analysis, Vertica, Vol. 5, pp. 99 to 129, 1981.

(7) I.C. Cheeseman — A Method of Calculating the Effect of One Helicopter Rotor Upon Another, A.R.C. Tech Report, C.P. 406, 1958.

(8) R.C. Dingeldein — Wind-Tunnel Studies of the Performance of Multi-Rotor Configurations NACA TN-3236, 1954.

(9) R.D. Harrington — Full-Scale Tunnel Investigation of the Static-Thrust Performance of a Coaxial Helicopter Rotor, NACA TN 2318, 1951.

(10) T. Nagashima, K. Nakanishi — Optimum Performance and Wake Geometry of Coaxial Rotor in Hover, Seventh European Rotorcraft Forum, 1981.

(11) M.J. Andrew — Coaxial Contrarotating Twin Rotor Aerodynamics, Ph.D. Thesis, Southampton University, 1983.

(12) H. Zimmer — The Aerodynamic Calculation of Counter Rotating Coaxial Rotors, Eleventh European Rotorcraft Forum, 1985.

(13) H. Azzam, P. Taylor — A prescribed Wake Model for Helicopter Rotor Behaviour, Eleventh European Rotorcraft Forum, 1985.

(14) J.D. Kocurek, J.L. Tangler — A Prescribed Wake Lifting Surface Hover Performance Analysis, Journal of the A.H.S. January 1977.

(15) S. Satio, A. Azuma — A Numerical Approach to Coaxial Rotor Aerodynamics, Seventh European Rotorcraft Forum, 1981.

(16) J.M. Pouradier, E. Horowitz — Aerodynamic Study of a Hovering Rotor, Vertica, Vol. 5, pp. 301-315, 1981.

(17) R.J. Huston — Wind Tunnel Measurements of Performance, Blade Motions and Blade Airloads for Tandem-Rotor Configurations With and Without Overlap, NASA TND-1971, 1963.

Acknowledgement

The support of Procurement Executive, Ministry of Defence is gratefully acknowledged.

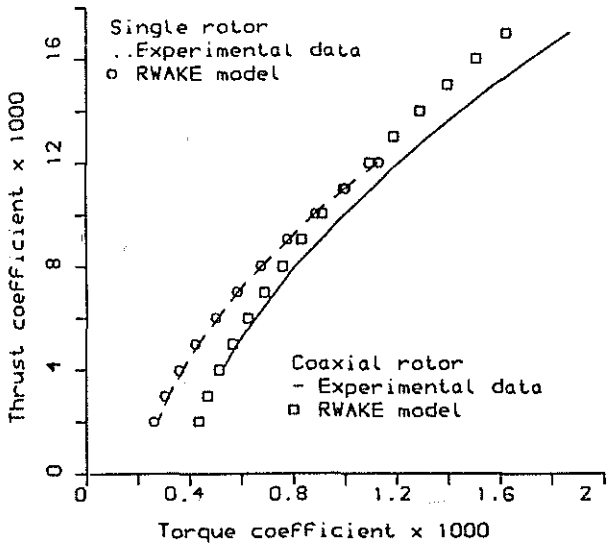

FIG.1 PERFORMANCE CURVE FOR COAXIAL ROTOR IN HOVER (Yawing moments are trimmed)

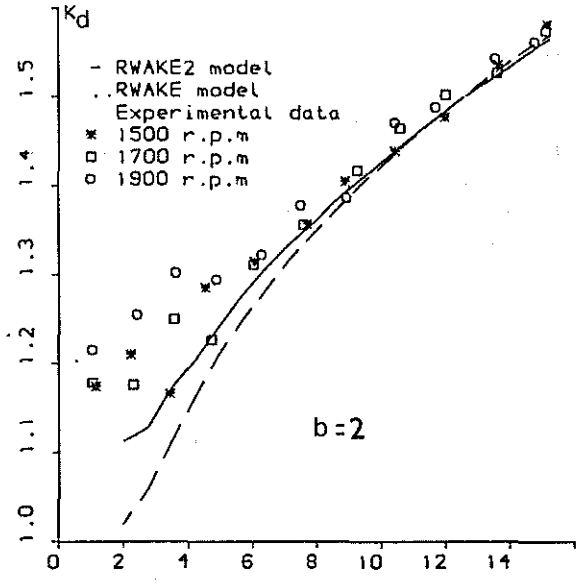

FIG.3 THE POWER FACTOR "K_d" IN HOVER

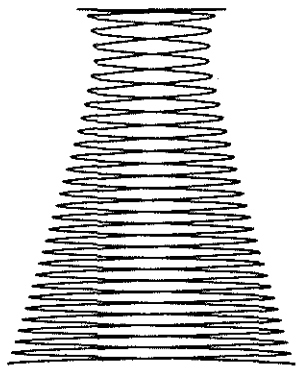

b=2

C_T=0.0086

(a) Hover

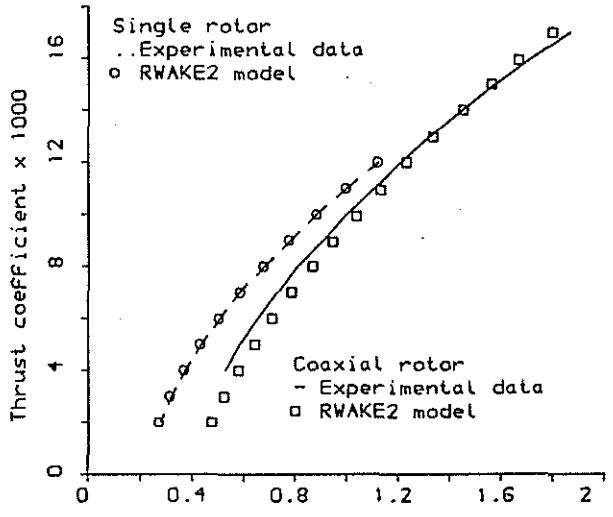

FIG.4 PERFORMANCE CURVE FOR COAXIAL ROTOR IN HOVER (Yawing moments are trimmed)

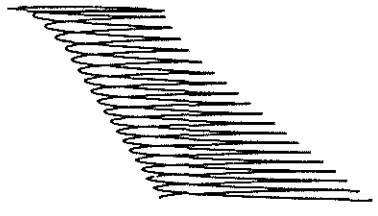

(b) advance ratio=0.04

FIG.2 PROPOSED TIP VORTEX TRAJECTORY

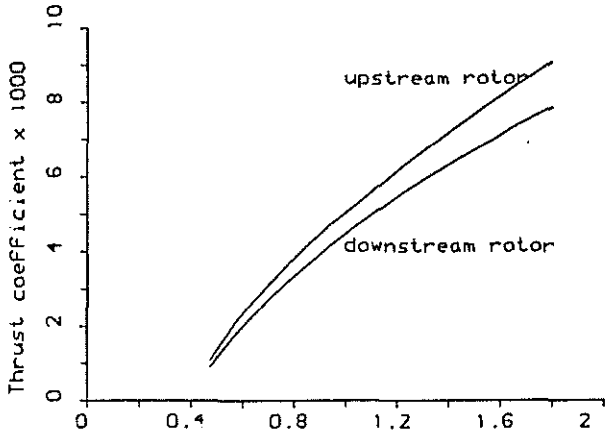

FIG.5 THRUST DISTRIBUTION OF COAXIAL ROTOR IN HOVER (Yawing moments are trimmed)

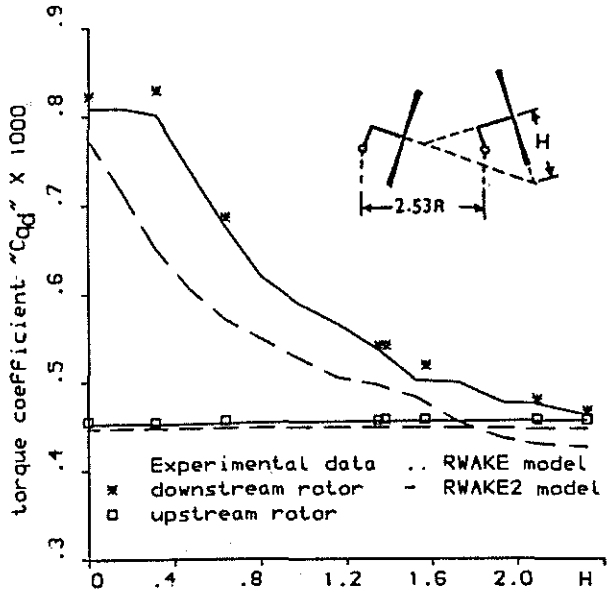

FIG.6 TORQUE VARIATION WITH DIHEDRAL TWIN-TAIL ROTOR IN HOVER

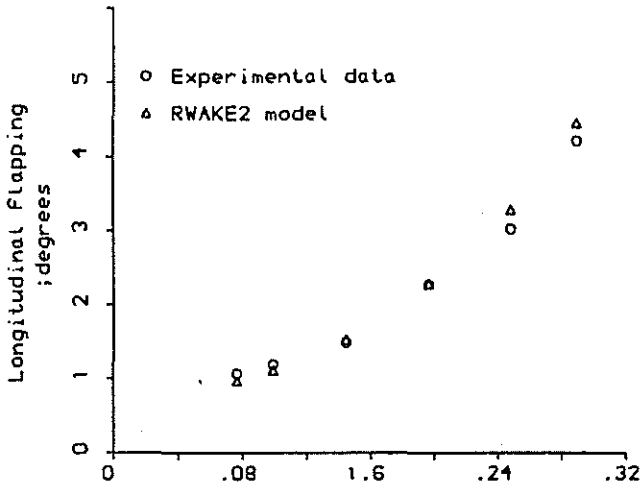

FIG.9 LONGITUDINAL FLAPPING OF A SINGLE ROTOR RELATIVE TO NONFEATHERING AXES

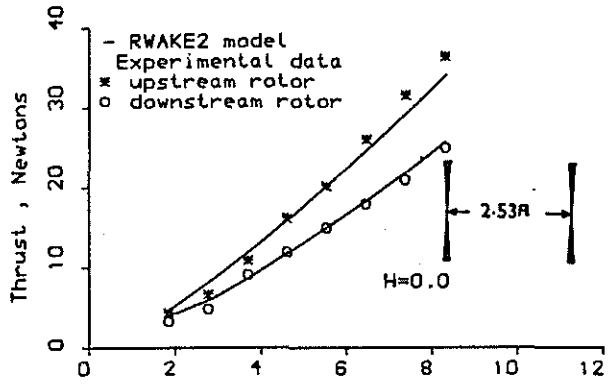

FIG.7 THRUST OF A TWIN-TAIL ROTOR AT ADVANCE RATIO OF 0.02

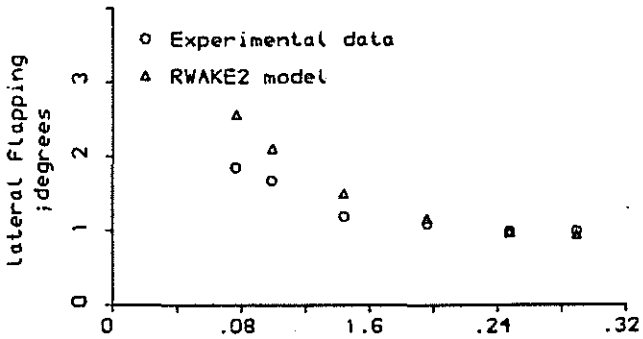

FIG.10 LATERAL FLAPPING OF A SINGLE ROTOR RELATIVE TO NONFEATHERING AXES

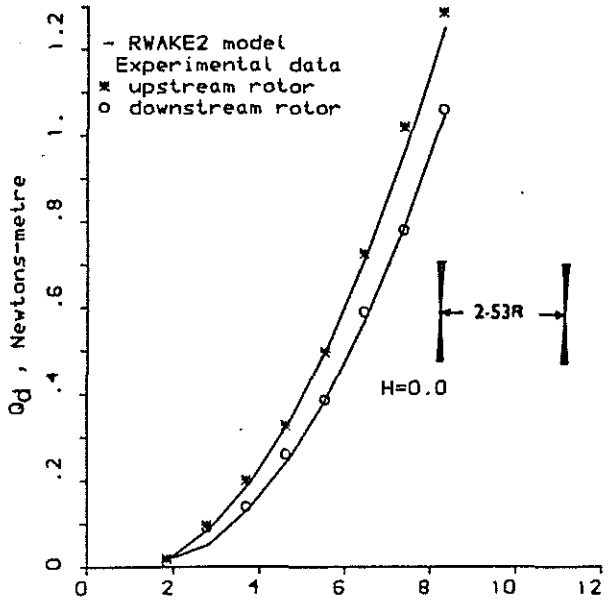

FIG.8 TORQUE OF A TWIN-TAIL ROTOR AT ADVANCE RATIO OF 0.02

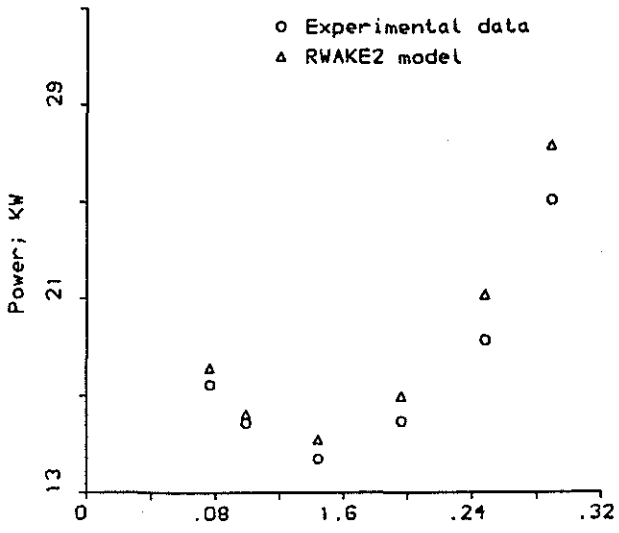

FIG.11 POWER OF A SINGLE TEETERING ROTOR

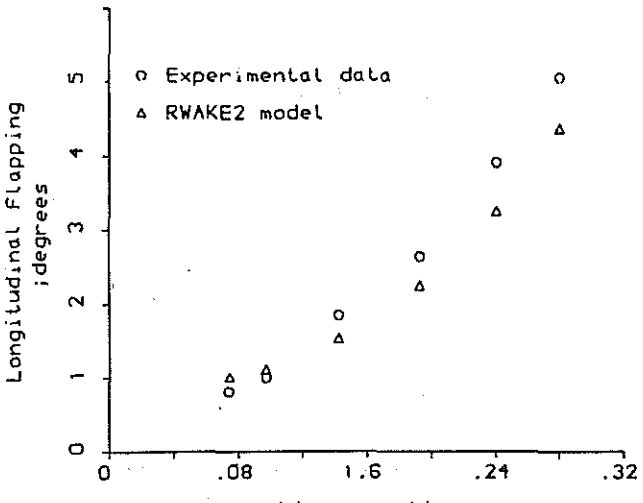

FIG.12 LONGITUDINAL FLAPPING OF A TANDEM ROTOR RELATIVE TO NONFEATHERING AXES; UPSTREAM ROTOR

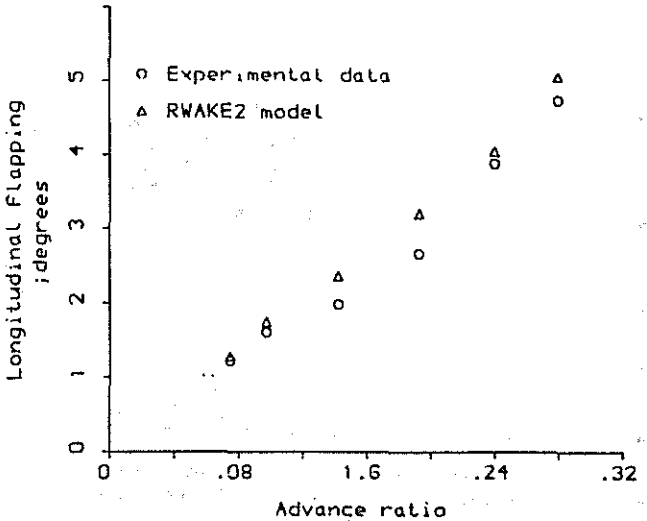

FIG.15 LONGITUDINAL FLAPPING OF A TANDEM ROTOR RELATIVE TO NONFEATHERING AXES; DOWNSTREAM ROTOR

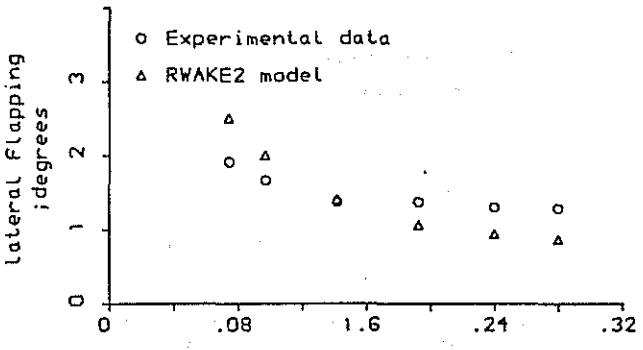

FIG.13 LATERAL FLAPPING OF A TANDEM ROTOR RELATIVE TO NONFEATHERING AXES; UPSTREAM ROTOR

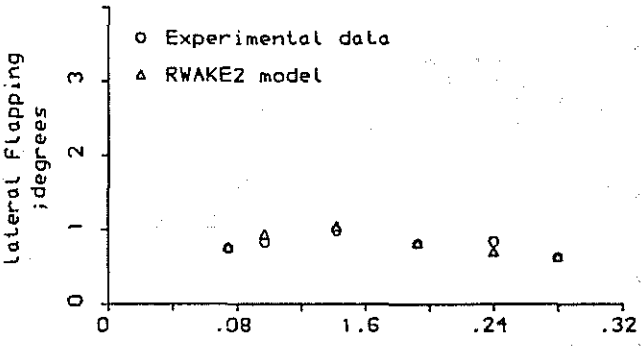

FIG.16 LATERAL FLAPPING OF A TANDEM ROTOR RELATIVE TO NONFEATHERING AXES; DOWNSTREAM ROTOR

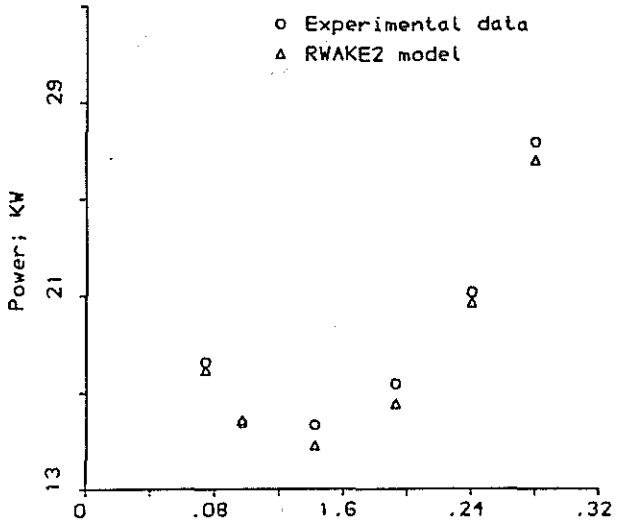

FIG.14 POWER OF A TANDEM ROTOR; UPSTREAM ROTOR

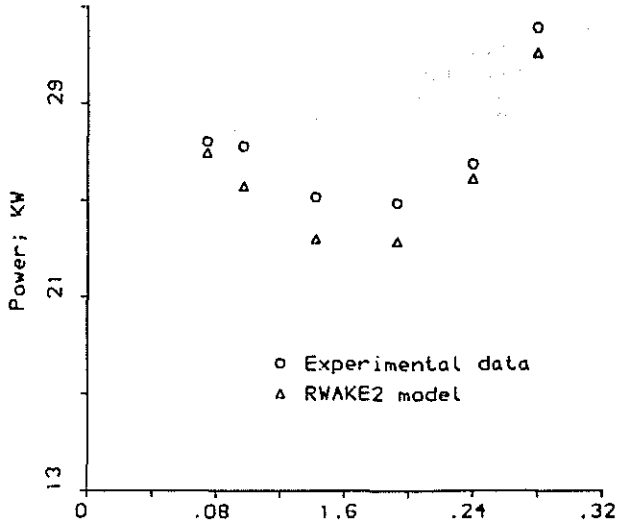

FIG.17 POWER OF A TANDEM ROTOR; DOWNSTREAM ROTOR